Use of the higher-order plate theory of I. N. Vekua type in problems of dynamics of heterogeneous plane waveguides

O. V. EGOROVA[1)], L. N. RABINSKIY[1)], S. I. ZHAVORONOK[2)]

[1)] *Faculty of Applied Mechanics, Moscow Aviation Institute (National Research University), 125993, 4 Volokolamskoe Shosse, Moscow, Russian Federation, e-mail: olha.egorova@yandex.ru*

[2)] *Department of Mechanics of Smart and Composite Materials and Systems, Institute of Applied Mechanics of Russian Academy of Sciences, 125040, 7 Leningradskiy Ave., Moscow, Russian Federation*

THE DYNAMICS OF ELASTIC PLANE WAVEGUIDES is studied on the basis of the extended formulation of the plate theory of Nth order. The plate model is based on the Lagrangian formalism of analytical dynamics combined with the dimensional reduction approach and the biorthogonal expansion of the spatial distribution of the displacement. The boundary conditions shifted from the faces onto the base plane are interpreted as constraints for the variational formulation of two-dimensional plate models. The normal wave dispersion in plates is modelled, the convergence of the approximate solutions is studied using the known exact solution for a plane layer as a reference. The proposed plate theory is used to analyse the normal wave dispersion in power graded waveguides of both symmetric and asymmetric structures, the locking phase frequencies for various power indices are computed.

Key words: thin-walled waveguides, plates, analytical dynamics, Lagrangian formalism, constraint equations, normal waves, phase frequencies, convergence.

1. Introduction

FUNCTIONALLY GRADED MATERIALS (hereinafter referred as FGM) were proposed primarily for the structures loaded by high temperatures to eliminate the drawback of layered materials consisting in their low delamination strength due to mismatches of thermal expansion factors of different layers [1, 2]. Plates or shells with the properties graded across the thickness are typical FG structures based on the composition of two constituents, the refractory ceramics and the metal [3]. The study of the behaviour of graded thin-walled structures remains topical nowadays; e.g. see [4-6]. In particular, the investigation of free vibrations [7] and harmonic wave dispersion in graded plate or shell structures is a basis for various non-destructive testing methods and for the estimation of the impact of structural defects on the strength and dynamics of FGMs, [8–11].

Only a few exact solutions for FGM shells of plates based on the three-dimensional elasticity theory are known, e.g. [12–18]. At the same time the classical Kirchhoff's and even the refined first-order shear deformation plate theories being still consistent with low-frequency oscillations of thin-walled FG structures [19–21] could fail in the high-frequency dynamics of FG plates. Moreover, in the same cases the classical models lead to the results that differ significantly from the ones offered by the "direct approach" due to the different ways of determination of the transverse shear stiffness, as it was shown in [7]. Indeed, most of plate models accounting for the transverse shear deals with the so-called "shear correction factor" that is not defined uniquely, [7, 22, 23]. The direct approach seems to be more reliable, but the known results are limited by the analysis of some lowest eigenvalues [7] for oscillating plates. On the other hand, the high frequency vibrations lead to some effects such as boundary layers near the faces [20].

The refinement of plate models consists in the accounting for higher kinematical degrees of freedom in addition to the translation and rotation of the middle surface point; e.g. see, [24–26]. Such models are useful for thin-walled FG structures, [27–31], but they are not free from some drawbacks; in particular, "...not in any case the boundary conditions on the upper and lower faces are fulfilled" [7]. Many methods can be used to refine plate and shell models; the asymptotic approach [32, 33] or [34] seems to be the most efficient way of the qualitative analysis of thin-walled structures, but it does not allow one to construct the complete hierarchies of solutions [35] that approximating three-dimensional solutions in various norms [36]. On the other hand, the finite element simulation [37] based on solid modelling remains the main approach in the practical engineering. The formal method of expansion of the displacement into series may be more efficient for the numerical simulation combined with the finite element [36] or meshless approaches [38]; as well a power series [20, 39–41], as a special function [28, 29, 42], could be used. In particular, the use of the Legendre polynomials as an expansion system allows one to obtain the reliable solutions for guided waves dynamics in functionally graded waveguides [43–47]. One of the universal approaches of construction of general higher-order is based on the generalized Fourier series [24, 25, 27, 36, 39]. Let us note also the sampling surface method [4, 48–51]; this formulation can be combined efficiently with a finite element simulation [52]. The application of the sampling surfaces approach to functionally graded structures is presented in [53].

An extended higher-order plate theory of I. N. Vekua type [24] is based on the well-studied dimensional reduction approach [24, 25, 27, 36, 39, 54–56] combined with the Lagrangian formalism of the analytical dynamics of constrained continuum systems. Such an approach leads to the interpretation of plate models as two-dimensional continua with sets of appropriate properties obtained from the reduction process [26, 55, 57]. Accordingly to [26], the model of a shell or a plate

is defined on the two-dimensional manifold corresponding to the base surface within the configuration space, the set of field variables, the surface and contour Lagrangian densities obtained from the spatial ones after the dimensional reduction (e.g. see [26, 57]) and the constraint equations. The field variables of the 1$^{\text{st}}$ kind are defined as biorthogonal expansion coefficients for the spatial distribution of the displacement vector field instead of the orthogonal series used earlier by [24, 25, 39, 55]. Such a formulation of a two-dimensional model is unified for different basis (Legendre polynomials, finite elements [26], etc.). The so-called "plate theory of N$^{\text{th}}$ order" results in the equations of motion having a regular structure; they could be efficiently derived using various computer algebra systems supporting main tensor algebra operations. The constraint equations appear as a result of shifting of the boundary conditions from the faces onto the base surface after the dimensional reduction [54, 58]. It is shown that the kinematic boundary conditions result in the holonomic constraints whereas the dynamic ones lead to the non-holonomic constraints [59]. The constrained problem can be solved by the Lagrange multiplier method [58] and allows one to obtain consistent low-order approximations [40]. Thus, the "extended", or "constrained" theory of plates allows one to eliminate the known drawback of higher order theories noted in [7].

The "extended" theory of plates is used to solve the problem of normal wave dispersion in functionally graded elastic plates. The convergence of solutions based on the plate theory of N$^{\text{th}}$ order was analysed. In [60], the Legendre polynomials were used as a basis, and in [61] for the "finite layer" variant of the plate model under the unified "elementary" formulation neglecting the constraints and leading to approximated wave reflection conditions on the faces; the analogous results for the extended formulation are shown below. Moreover, the wave dispersion in both symmetrically and asymmetrically power-graded elastic layers is investigated on the basis of the extended plate theories of various orders, and the locking frequencies for different power indices are computed.

2. Variational formulation of the higher-order plate theory based on the analytical dynamics of 2D continua and the finite element discretization

Let us consider the plate as a three-dimensional body $V \in \mathbb{R}^3$ bounded by face planes $S_\pm$ and piecewise-smooth lateral surface S_B, $\partial V = S_\pm \oplus S_B$, [26, 57, 58] and let us introduce the base plane S with curvilinear coordinates $\xi^\alpha \in D_\xi \subset \mathbb{R}^2$, $\alpha = 1, 2$:

$$\forall M \in S \quad \mathbf{r}(M) = \mathbf{r}(\xi^1, \xi^2).$$

Let us define the normal coordinate $\xi^3 \in [h_-, h_+]$ where $h_\pm$ corresponds to upper and lower faces of the plate, respectively:

$$\forall M_\pm \in S_\pm \quad \mathbf{R}(M_\pm) = \mathbf{r}(\xi^1, \xi^2) + h_\pm \mathbf{n},$$

therefore

$$\forall M\prime \in \bar{V} \quad \mathbf{R}(M\prime) = \mathbf{r}(\xi^1, \xi^2) + \xi^3 \mathbf{n},$$

where $\mathbf{n}$ is the normal unit vector at a point $M \in S$:

$$\mathbf{n} = \frac{\mathbf{r}_1 \times \mathbf{r}_2}{\sqrt{a}}, \quad \mathbf{r}_\alpha = \frac{\partial \mathbf{r}(\xi^1, \xi^2)}{\partial \xi^\alpha}, \quad a = \det a_{\alpha\beta}, \quad a_{\alpha\beta} = \mathbf{r}_\alpha \cdot \mathbf{r}_\beta,$$

here $\mathbf{r}_\alpha$ are covariant base vectors on the plane S and $a_{\alpha\beta}$ is the covariant metrics while the symbols "·" and "×" denote the dot and cross products, respectively. Thus, the displacement vector field can be referred to the contravariant vector triad $\mathbf{r}^\beta = a^{\alpha\beta}\mathbf{r}_\beta$, $\mathbf{n}$:

$$(2.1) \qquad \mathbf{u}(M\prime, t) = u_\alpha(\xi^1, \xi^2, \xi^3, t)\mathbf{r}^\alpha(\xi^1, \xi^2) + u_3(\xi^1, \xi^2, \xi^3, t)\mathbf{n}.$$

The dynamics of the elastic body $\bar{V}$ could be defined by Hamilton's principle [26]:

$$(2.2) \qquad \delta \mathcal{H} = 0, \quad \mathcal{H} = \int\limits_{t_0}^{t_1} \left(\int\limits_V \mathcal{L}_V(\mathbf{u}, \dot{\mathbf{u}}, \nabla \otimes \mathbf{u}) dV + \int\limits_{\partial V} \mathcal{L}_{\partial V}(\mathbf{u}) dS \right) dt,$$

$$\mathbf{u}|_{t=t_0} = \mathbf{u}_0, \quad \dot{\mathbf{u}}|_{t=t_0} = \mathbf{v}_0,$$

here and below $\dot{\mathbf{u}} \equiv \partial \mathbf{u}/\partial t$, $t \in [0, \infty)$ is the time parameter, $\nabla = \mathbf{r}^\beta \partial_\beta + \mathbf{n}\partial_3$ is the "nabla" operator, the symbol "$\otimes$" denotes the tensor product. The volumetric density of the Lagrangian $\mathcal{L}_V$ and the surface density $\mathcal{L}_{\partial V}$ are defined as follows:

$$(2.3) \qquad \mathcal{L}_V(\mathbf{u}, \dot{\mathbf{u}}, \nabla \otimes \mathbf{u}) = \frac{1}{2}\rho\dot{\mathbf{u}} \cdot \dot{\mathbf{u}} - \frac{1}{2}(\nabla \otimes \mathbf{u})^{\mathrm{T}} : \mathbf{C} : (\nabla \otimes \mathbf{u}) + \rho\mathbf{F} \cdot \mathbf{u},$$

$$\mathcal{L}_{\partial V}(\mathbf{u}) = \mathbf{q}_\pm \cdot \mathbf{u}|_{M \in S_\pm} + \mathbf{q}_B \cdot \mathbf{u}|_{M \in S_B},$$

ρ is the mass density, $\mathbf{C}$ is the elasticity tensor, $\mathbf{F}$ is the bulk force vector, and $\mathbf{q}_\pm$, $\mathbf{q}_B$ are resultant force vectors on the faces $S_\pm$ and on the lateral surface S_B, respectively.

A two-dimensional plate model could be interpreted as a "material surface" furnished by a set of appropriate mechanical properties, e. g. tangent and bending stiffness, transverse shear stiffness, and several higher-order quantities. Such a treatment is quite similar to the "direct approach" proposed in [62] and to two-dimensional Cosserat continuum models [63, 64]. Contrarily to these ones, all mechanical properties are defined as a result of the dimensional reduction of the three-dimensional variational problem given by (2.2) and (2.3).

On the other hand, the two-dimensional plate model is a continuum Lagrangian system that could be defined within a configuration space $\Omega = \{\mathbf{u}^{(k)}\}$

with a set of field variables $\mathbf{u}^{(k)}$, $k \in \mathbb{N} \cup \{\emptyset\}$, the correspoding densities of the Lagrangian $\mathcal{L}_S(\mathbf{u}^{(k)}, \dot{\mathbf{u}}^{(k)}, \bar{\nabla} \otimes \mathbf{u}^{(k)})$, $\mathcal{L}_\Gamma(\mathbf{u}^{(k)})$ defined on the plane S and the contour $\Gamma = S \cap S_B$ [26, 57, 60] and by some constraint equations $\mathbf{f}(\mathbf{u}^{(k)}, \bar{\nabla} \otimes \mathbf{u}^{(k)}) = 0$. Here and below $\bar{\nabla} = \mathbf{r}^\alpha \partial_\alpha$ denotes the "nabla" opterator on the plane S. The dynamics of a plate is given by the Hamilton principle:

$$(2.4) \qquad \delta \int_{t_0}^{t_1} \left[\int_S \mathcal{L}_S(\mathbf{u}^{(k)}, \dot{\mathbf{u}}^{(k)}, \bar{\nabla} \otimes \mathbf{u}^{(k)}) dS + \int_{\partial S} \mathcal{L}_\Gamma d\Gamma \right] dt = 0,$$

$$\mathbf{u}^{(k)}|_{t=t_0} = \mathbf{u}_0^{(k)}, \quad \dot{\mathbf{u}}^{(k)}|_{t=t_0} = \mathbf{v}_0^{(k)}.$$

The dimensional reduction [24, 25, 27, 54] offers an efficient way to construct the variational formulation (2.4) of the two-dimensional plate model on the basis of the three-dimensional problem statement (2.2). Let us consider the biorthogonal system $\mathrm{p}_{(k)}(\zeta)$, $\mathrm{p}^{(k)}(\zeta)$, where $\zeta \in [-1, 1]$ is the dimensionless normal coordinate:

$$(\mathrm{p}_{(k)}, \mathrm{p}^{(m)})_1 \equiv \int_{-1}^{1} \mathrm{p}_{(k)}(\zeta) \mathrm{p}^{(m)}(\zeta) d\zeta = \delta_{(k)}^{(m)},$$

$$\zeta = 2\big[\xi^3 - \tfrac{1}{2}(h_+ + h_-)\big]/(h_+ - h_-),$$

and let us assume the components $u_\alpha(\xi^1, \xi^2, \zeta, t)$ and $u_3(\xi^1, \xi^2, \zeta, t)$ be square integrable over $[-1, 1] \ni \zeta$. Thus, the three-dimensional displacement field (2.1) could be defined as follows:

$$(2.5) \qquad \mathbf{u}(\xi^1, \xi^2, \zeta, t) = \mathbf{u}^{(k)}(\xi^1, \xi^2, t) \mathrm{p}_{(k)}(\zeta)$$

$$\equiv [u_\alpha^{(k)}(\xi^1, \xi^2, t) \mathbf{r}^\alpha + u_3^{(k)}(\xi^1, \xi^2, \zeta) \mathbf{n}] \mathrm{p}_{(k)}(\zeta),$$

$$(2.6) \qquad u_\alpha^{(k)} = (u_\alpha, \mathrm{p}^{(k)})_1, \quad u_3^{(k)} = (u_3, \mathrm{p}^{(k)})_1.$$

As a result, we can reduce the volumetric and boundary densities of the Lagrangian to its surface and contour densities [57]; for an orthotropic plate we have

$$(2.7) \qquad \mathcal{L}_S(u_\alpha^{(k)}, \dot{u}_\alpha^{(k)}, \nabla_\beta u_\alpha^{(k)}, u_3^{(k)}, \dot{u}_3^{(k)}, \nabla_\beta u_3^{(k)})$$

$$= \frac{1}{2} \rho_{(k)}^{(m)} (\dot{u}_{(m)}^\alpha \dot{u}_\alpha^{(k)} + \dot{u}_{(m)}^3 \dot{u}_3^{(k)}) + F_{(k)}^\alpha u_\alpha^{(k)} + F_{(k)}^3 u_3^{(k)}$$

$$- \frac{1}{2} (C_{(km)}^{\alpha\beta\gamma\delta} \nabla_\delta u_\gamma^{(m)} + h^{-1} C_{(kn)}^{\alpha\beta33} D_{(m\cdot)}^{(\cdot n)} u_3^{(m)}) \nabla_\beta u_\alpha^{(k)}$$

$$- \frac{1}{2h} (C_{(lm)}^{33\gamma\delta} \nabla_\delta u_\gamma^{(m)} + h^{-1} C_{(ln)}^{3333} D_{(m\cdot)}^{(\cdot n)} u_3^{(m)}) D_{(k\cdot)}^{(\cdot l)} u_3^{(k)}$$

$$- \frac{1}{2h} C_{(km)}^{3\alpha3\beta} (\nabla_\beta u_3^{(m)} + h^{-1} D_{(n\cdot)}^{(\cdot m)} u_\beta^{(n)})(\nabla_\beta u_3^{(k)} + h^{-1} D_{(n\cdot)}^{(\cdot k)} u_\beta^{(n)}),$$

$$\mathcal{L}_\Gamma = q_{(k)B}^\alpha u_\alpha^{(k)} + q_{(k)B}^3 u_3^{(k)},$$

The linear operators used in (2.7) are introduced following [26], [57]:

$$
\begin{aligned}
D_{(n\cdot)}^{(\cdot k)} &= (d\mathrm{p}_{(n)}/d\zeta, \mathrm{p}^{(k)})_1, \\
\rho_{(k)}^{(m)} &= (\rho\mathrm{p}^{(m)}, \mathrm{p}_{(k)})_1, \\
C_{(km)}^{ijpq} &= (C^{ijpq}\mathrm{p}_{(k)}, \mathrm{p}_{(m)})_1,
\end{aligned}
$$
(2.8)

here C^{ijkl} are the contravariant components of the elasticity tensor $\mathbf{C}$.

The resultant force vector components on the plate contour are introduced in [26]:

$$
q_{B(k)}^{i} = (q^i|_{M \in S_B}, \mathrm{p}_{(k)})_1.
$$

The initial conditions can be written as follows:

(2.9) $\quad u_{(k)}^{\alpha}|_{t=t_0} = U_{(k)}^{\alpha}; \quad \dot{u}_{(k)}^{\alpha}|_{t=t_0} = V_{(k)}^{\alpha}, \quad u_{(k)}^{3}|_{t=t_0} = U_{(k)}^{3}, \quad \dot{u}_{(k)}^{\alpha}|_{t=t_0} = V_{(k)}^{3}.$

The biorthogonal expansion coefficients $\mathbf{u}^{(k)}$ can be interpreted hence as field variables of the first kind [26, 57]. For the linear system (2.2), (2.3) the further reduction of the three-dimensional problem consists in the projection of the configuration space Ω onto its subspace Ω_N $(k = 0, 1, \ldots, N)$ [26]. As a result, the dynamics of the plate is approximated by $N + 1$ vector degrees of freedom $\mathbf{u}^{(k)}$. The equations of motion of the so-called plate theory of N$^{\mathrm{th}}$ order can be derived as Lagrange equations of the second kind for the two-dimensional continuum system given by (2.4), (2.7), (2.9) (see [26, 57], and [60]):

(2.10) $\qquad \rho_{(km)}\ddot{u}^{\alpha(m)} = C_{(km)}^{\alpha\beta\gamma\delta}\nabla_\beta\nabla_\delta u_\gamma^{(m)} - h^{-2}D_{(k\cdot)}^{(\cdot n)}C_{(ns)}^{\alpha 33\,\gamma}\bar{D}_{(m\cdot)}^{(\cdot s)}u_\gamma^{(m)}$

$\qquad\qquad - h^{-1}[D_{(k\cdot)}^{(\cdot n)}C_{(nm)}^{\alpha 33\beta} - C_{(kn)}^{\alpha\beta 3\,3}\bar{D}_{(m\cdot)}^{(\cdot n)}]\nabla_\beta u_3^{(m)},$

(2.11) $\qquad \rho_{(km)}\ddot{u}^{3(m)} = C_{(km)}^{3\beta 3\delta}\nabla_\beta\nabla_\delta u_3^{(m)} - h^{-2}D_{(k\cdot)}^{(\cdot n)}C_{(ns)}^{3333}\bar{D}_{(m\cdot)}^{(\cdot s)}u_3^{(m)}$

$\qquad\qquad - h^{-1}[D_{(k\cdot)}^{(\cdot n)}C_{(nm)}^{33\gamma\beta} - C_{(km)}^{3\beta 3\gamma}\bar{D}_{(k\cdot)}^{(\cdot n)}]\nabla_\beta u_\gamma^{(m)}.$

Their natural boundary conditions can be written in the following notation [57]:

(2.12) $\qquad [(C_{(km)}^{\alpha\beta\gamma\delta}\nabla_\delta u_\gamma^{(m)} + C_{(km)}^{\alpha\beta 3}u_3^{(m)})\nu_\beta - q_{(k)}^\alpha]\delta u_\alpha^{(k)}|_\Gamma = 0,$

(2.13) $\qquad [(C_{(km)}^{3\beta 3\delta}\nabla_\delta u_3^{(m)} + C_{(km)}^{3\beta\gamma}u_\gamma^{(m)})\nu_\beta - q_{(k)}^3]\delta u_3^{(k)}|_\Gamma = 0.$

The initial-boundary value problem statement (2.9)–(2.13) corresponds to the so-called "elementary" plate theory of the N$^{\mathrm{th}}$ order that allows one to fulfil the boundary conditions on the faces $S_\pm$ after solution's convergence at the end points $\zeta = \pm 1$. To satisfy the boundary conditions exactly we should use the "extended" theory of plates proposed in [58].

Let us consider the dynamic boundary conditions on the faces $S_\pm$ corresponding to the three-dimensional statement of the elasticity theory:

(2.14)
$$(C^{33\gamma\delta}\nabla_\delta u_\gamma + h^{-1}C^{3333}\partial_\zeta u_3)|_{\zeta=\pm1} = q_\pm^3,$$
$$C^{\alpha3\beta3}(\nabla_\beta u_3 + h^{-1}u_\beta)|_{\zeta=\pm1} = q_\pm^\alpha.$$

Substituting the expansions (2.5) into the boundary conditions (2.14) and taking into account the formulae (2.8), we obtain the following relations [58]:

(2.15)
$$C_{(km)}^{\alpha3\delta3}(\nabla_\delta u_3^{(k)} + h^{-1}D_{(m\cdot)}^{(\cdot k)}u_\delta^{(m)})\mathrm{p}^{(m)}(\pm1) \pm q_\pm^\alpha = 0;$$
$$(C_{(km)}^{33\gamma\delta}\nabla_\delta u_\gamma^{(k)} + h^{-1}C_{(km)}^{3333}D_{(n\cdot)}^{(\cdot k)}u_3^{(n)})\mathrm{p}^{(m)}(\pm1) \pm q_\pm^3 = 0.$$

The equations (2.15) are defined on the base plane S and expressed through the field variables of the 1st kind $u_i^{(k)}$ and their covariant derivatives, therefore they could be interpreted as non-holonomic constraint equations for the Lagrangian two-dimensional system (2.4), (2.7), (2.9). Thus, the plate model allowing one to fulfil the boundary conditions on the faces $S_\pm$ becomes constrained; the approproate dynamic equations and natural boundary conditions can be derived using the Lagrange multiplier method [58, 59]. However, an alternative approach for spectral problems is shown below. Let us note that the kinematic boundary conditions result in the holonomic constraints [59].

Let us also note that the unified formulation (2.4)–(2.9) of the plate theory of Nth order presented above is invariant on the used base system $\mathrm{p}_{(k)}(\zeta)$; one can use as well the orthogonal base functions, e.g. the Legendre polynomials, as the piecewise-linear compact functions corresponding to the finite element discretization ("finite layer" model) [61]:

$$\mathrm{p}_{(0)}(\zeta) = p_{(0,1)}(\zeta), \ \ldots, \ \mathrm{p}_{(k)}(\zeta) = p_{(k,2)}(\zeta) + p_{(k+1,1)}(\zeta),$$
$$k = 1, 2, \ldots N - 1,$$
$$\ldots \ \ \mathrm{p}_{(N)}(\zeta) = p_{(N,2)}(\zeta),$$

(2.16)
$$p_{(k,1)} = \begin{cases} \dfrac{\zeta - \zeta_{k+1}}{\zeta_{k+1} - \zeta_k}, & \zeta \in [\zeta_k, \zeta_{k+1}], \\ 0, & \zeta \notin [\zeta_k, \zeta_{k+1}], \end{cases}$$
$$p_{(k,2)} = \begin{cases} \dfrac{\zeta - \zeta_k}{\zeta_{k+1} - \zeta_k}, & \zeta \in [\zeta_k, \zeta_{k+1}], \\ 0, & \zeta \notin [\zeta_k, \zeta_{k+1}], \end{cases}$$
$$\zeta_k = h_- + N^{-1}(h_+ - h_-), \quad k = 0, 1, \ldots, N + 1.$$

The Shauder basis allows one to consider the classical plate model with two degrees of freedom at each point of the base surface, the translation and the rotation, enriched by the finite element discretization. These three types of base functions are shown in Fig. 1.
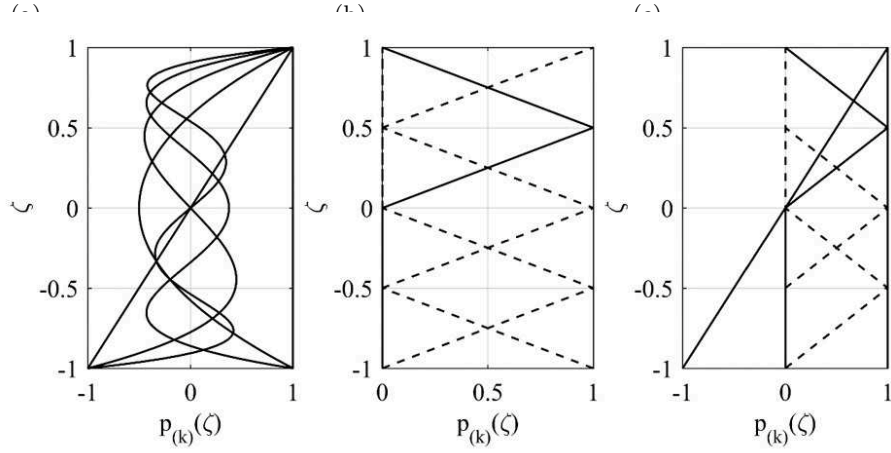
FIG. 1. Various base systems $p_{(k)}(\zeta)$ used within an unified formulation of the plate theory of Nth order: Legendre polynomials (a), piecewise linear shape functions (b), combined model given by Shauder basis (c).

3. Modelling of the normal wave dispersion in elastic plates on the basis of the extended plate theory of Nth order

Let us consider a layer of thickness $2h$ referred to the Cartesian frame $Ox^1x^2x^3$. The material is assumed to be ideally elastic and graded across the thickness; $E(\zeta)$ is the Young modulus, ν is the Poisson ratio, $\mu(\zeta)$ is the shear modulus and $\rho(\zeta)$ is the mass density. Thus, we obtain the following stiffness and mass properties for the plate:

$$C_{(km)}^{\alpha\beta\gamma\delta} = \lambda_{(km)}a^{\alpha\beta}a^{\gamma\delta} + \mu_{(km)}(a^{\alpha\gamma}a^{\beta\delta} + a^{\alpha\delta}a^{\beta\gamma}), \quad C_{(km)}^{\alpha3\beta3} = \mu_{(km)}a^{\alpha\beta},$$

$$C_{(km)}^{3333} = \lambda_{(km)} + 2\mu_{(km)}, \quad C_{(km)}^{\alpha\beta33} = \lambda_{(km)}a^{\alpha\beta}, \quad E_{(km)} = (E(\zeta)\mathrm{p}_{(k)},\mathrm{p}_{(m)})_1$$

$$\lambda_{(km)} = \nu E_{(km)}(1-2\nu)^{-1}(1+\nu)^{-1}, \quad \mu_{(km)} = \tfrac{1}{2}E_{(km)}(1+\nu)^{-1},$$

$$\rho_{(km)} = (\rho(\zeta)\mathrm{p}_{(k)},\mathrm{p}_{(m)})_1.$$

The example of a typical power graded plate with two constituents, the ceramics and the metal (e. g. see [65]), is considered below; so, the elastic moduli of the constituents are denoted hereinafter as E_C, E_M, and the corresponding mass densities as ρ_C, ρ_M. We can define the Young modulus and the mass density at a point ζ by the following formulae:

$$(3.1) \quad E(\zeta) = E_C[\tilde{E}_M + q(\zeta)\Delta\tilde{E}], \quad \tilde{E}_M = E_C^{-1}E_M, \quad \Delta\tilde{E} = E_C^{-1}(E_C - E_M),$$

$$(3.2) \quad \rho(\zeta) = \rho_C[\tilde{\rho}_M + q(\zeta)\Delta\tilde{\rho}], \quad \tilde{\rho}_M = \rho_C^{-1}\rho_M, \quad \Delta\tilde{\rho} = \rho_C^{-1}(\rho_C - \rho_M).$$

Accordingly to [60] and [61], let us introduce the following dimensionless coordinate $\xi = x_1 h^{-1}$, time $\tau = tc_2 h^{-1}$, and field variable $\tilde{u}_\alpha^{(k)} = u_\alpha^{(k)} h^{-1}$;

$c_2 = \sqrt{\rho_{\mathrm{C}}^{-1}\mu_{\mathrm{C}}}$ denotes the shear wave velocity in the pure ceramics. Thus, accounting for the homogeneous boundary conditions, $q_{\pm}^i = 0$ and for the absence of bulk forces, $F_{(k)}^i = 0$, we obtain the following dimensionless equations of motion corresponding to (2.10), (2.11) [61]:

$$
R_{(km)}\partial_\tau^2 u_1^{(m)} = \beta^{-2}V_{(km)}\partial_\xi^2 u_1^{(m)} - D_{(k\cdot)}^{(\cdot n)}V_{(ns)}\bar{D}_{(m\cdot)}^{(\cdot s)}u_1^{(m)}
$$
$$
- [D_{(k\cdot)}^{(\cdot n)}V_{(nm)} - (\beta^{-2} - 2)V_{(kn)}\bar{D}_{(m\cdot)}^{(\cdot n)}]\partial_\xi u_2^{(m)},
$$
$$
R_{(km)}\partial_\tau^2 u_2^{(m)} = V_{(km)}\partial_\xi^2 u_2^{(m)} + \beta^{-2}D_{(k\cdot)}^{(\cdot n)}V_{(ns)}\bar{D}_{(m\cdot)}^{(\cdot s)}u_2^{(m)}
$$

(3.3)
$$
- [(\beta^{-2} - 2)D_{(k\cdot)}^{(\cdot n)}V_{(nm)} - V_{(kn)}\bar{D}_{(m\cdot)}^{(\cdot n)}]\partial_\xi u_1^{(m)},
$$
$$
c_1 = \sqrt{\rho_{\mathrm{C}}^{-1}(\lambda_C + 2\mu_C)}, \quad \beta^2 = c_1^{-2}c_2^2,
$$
$$
V_{(km)} = \tilde{E}G_{(km)} + \Delta\tilde{E}Q_{(km)},
$$
$$
R_{(km)} = \tilde{\rho}G_{(km)} + \Delta\rho Q_{(km)},
$$
$$
Q_{(km)} = (q(\zeta)\mathrm{p}_{(k)}, \mathrm{p}_{(m)})_1, \quad G_{(km)} = (\mathrm{p}_{(k)}, \mathrm{p}_{(m)})_1.
$$

Let the normal wave propagate along the axis $O\xi$:

(3.4)
$$
\mathbf{u}^{(k)} = \mathbf{U}^{(k)}\exp[i(\kappa\xi - \omega\tau)], \quad i = \sqrt{-1},
$$

$\tilde{\omega} = \omega h/c_2$ is the dimensionless phase frequency (tildes are omitted hereinafter) and $\kappa = kh$ is the dimensionless wavenumber whereas $\mathbf{U}^{(k)}$ denotes the amplitude. Substitution of (3.4) into the equations of motion (3.3) results in the spectral problem analogous to [60, 61]:

(3.5)
$$
|\mathbf{A} - \omega^2\mathrm{P}| = 0,
$$

(3.6) $\mathbf{A} =$

$$
\begin{pmatrix}
\kappa^2\beta^{-2}V_{(km)} + D_{(k\cdot)}^{(\cdot n)}V_{(ns)}\bar{D}_{(m\cdot)}^{(\cdot s)} & i\kappa[D_{(k\cdot)}^{(\cdot n)}V_{(nm)} - (\beta^{-2} - 2)V_{(kn)}\bar{D}_{(m\cdot)}^{(\cdot n)}] \\
i\kappa[(\beta^{-2} - 2)D_{(k\cdot)}^{(\cdot n)}V_{(nm)} - V_{(kn)}\bar{D}_{(m\cdot)}^{(\cdot n)}] & \kappa^2 V_{(km)} + \beta^{-2}D_{(k\cdot)}^{(\cdot n)}V_{(ns)}\bar{D}_{(m\cdot)}^{(\cdot s)}
\end{pmatrix},
$$

(3.7)
$$
\mathbf{P} = \begin{pmatrix} R_{(km)} & 0 \\ 0 & R_{(km)} \end{pmatrix}.
$$

The spectral problem given by (3.5)–(3.7) corresponds to the "elementary" plate theory. To fulfil the boundary conditions on $S_\pm$ we have to consider also the constraint equations; substitution of (3.4) into Eqs. (2.15) results in the following linear constraints [66]:

(3.8)
$$
\mathbf{B}\cdot\mathbf{U} = 0, \quad \mathbf{B} = (\mathbf{B}_+ \ \ \mathbf{B}_-)^{\mathrm{T}},
$$

(3.9) $\mathbf{B}_\pm = \begin{pmatrix} i\kappa(\beta^{-2} - 2)V_{(km)}\mathrm{p}^{(m)}(\pm 1) & \beta^{-2}V_{(mn)}\bar{D}_{(k\cdot)}^{(\cdot n)}\mathrm{p}^{(m)}(\pm 1) \\ V_{(mn)}\bar{D}_{(k\cdot)}^{(\cdot n)}\mathrm{p}^{(m)}(\pm 1) & i\kappa V_{(km)}\mathrm{p}^{(m)}(\pm 1) \end{pmatrix}.$

We could obtain hence the phase frequencies from the solution of the constrained stationary values problem for two quadratic forms $\mathbf{A}$ and $\mathbf{P}$ accordingly to [67]:

$$(3.10) \qquad \frac{\mathbf{U}^{\mathrm{T}} \cdot \mathbf{A} \cdot \mathbf{U}}{\mathbf{U} \cdot \mathbf{P} \cdot \mathbf{U}} = 0, \quad \mathbf{B} \cdot \mathbf{U} = 0.$$

Following [76], let us introduce the QZ decomposition for the constraint matrix (3.9)

$$\mathbf{Q}^{\mathrm{T}} \cdot \mathbf{B}^{\mathrm{T}} \cdot \mathbf{Z} = \begin{pmatrix} \mathbf{S} & \mathbf{0} \\ \mathbf{0} & \mathbf{0} \end{pmatrix}_{(2N+2)\times 4},$$

As a result, we obtain the following operator accounting for the constraints (3.8):

$$(3.11) \qquad \mathbf{A}_C = \mathbf{Q}^{\mathrm{T}} \cdot \mathbf{A} \cdot \mathbf{Q},$$

$$\mathbf{A}_C = \begin{pmatrix} \bar{\mathbf{A}}_{11} & \bar{\mathbf{A}}_{12} \\ \bar{\mathbf{A}}_{21} & \bar{\mathbf{A}}_{22} \end{pmatrix}_{(2N+2)\times(2N+2)},$$

and the stationary values ω_k for the pair $\mathbf{A}, \mathbf{P}$ can be found from the unconstrained problem:

$$(3.12) \qquad (\bar{\mathbf{A}}_{22} - \omega^2 \bar{\mathbf{P}}_{22}) \cdot \bar{\mathbf{U}} = 0, \quad \bar{\mathbf{U}} = \mathbf{Q}^{\mathrm{T}} \cdot \mathbf{U}.$$

The eigenvectors corresponding to the eigenvalue ω_k are defined as follows:

$$(3.13) \qquad \mathbf{U}^k = \mathbf{Q} \cdot [0\ 0\ 0\ 0\ \bar{U}_1^{k(m)}\ \bar{U}_3^{k(m)}]^T, \quad k \in [1, 2N-2] \cap \mathbb{Z}.$$

4. Convergence analysis: the homogeneous isotropic plate

The convergence analysis can be performed on the basis of the well-known analytical solution for the wave dispersion problem in an isotropic homogeneous layer based on the elasticity theory; this solution for the phase frequencies is used hereinafter as a reference, and the solution of the constrained spectral problem (3.10) of the plate theory of Nth order where $q(\zeta) \equiv 1$, $V_{(mn)} = R_{(mn)} = G_{(mn)}$. The spectrum of the system consists in two subspectra S and A corresponding to the longitudinal and bending waves in the layer [66]:

$$S : k, m = \{2n,\ N+2n\},\ A : k, m = \{2n-1,\ N+2n-2\},\ n \in \left[0, \left[\tfrac{1}{2}(N-1)\right]\right] \cup \mathbb{Z},$$

and the waveforms can be defined in terms of the plate theory as follows [67]:

$$(4.1) \qquad u_1^n(\zeta) = U_1^{k(m)} p_{(m)}(\zeta), \quad u_3^n(\zeta) = U_3^{k(m)} p_{(m)}(\zeta).$$
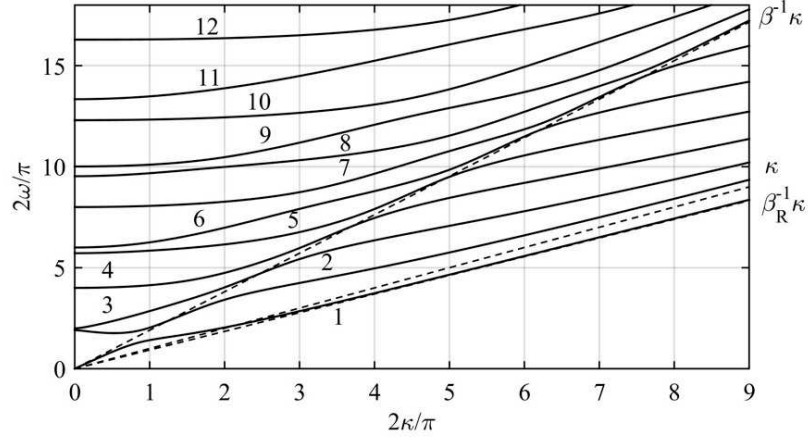
Fig. 2. Phase frequencies $2\omega/\pi$ of longitudinal modes, $k, m = \{2n, N + 2n + 2\}$, $n \in \left[0, \left[\frac{1}{2}(N+1)\right]\right] \cup \bowtie$, extended plate theory of 16th order.
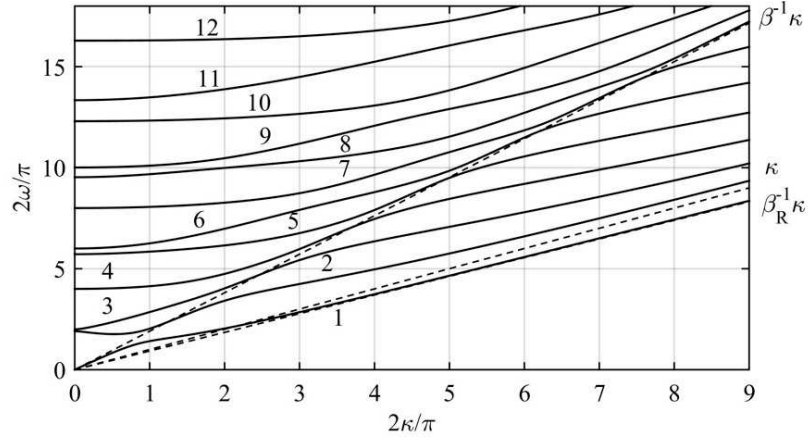
Fig. 3. Phase frequencies $2\omega/\pi$ of longitudinal modes, $\beta = c_2/c_1$, $\beta_R = c_R/c_1$, $k, m = \{2n + 1, N + 2n\}$, $n \in \left[0, \left[\frac{1}{2}(N+1)\right]\right] \cup \bowtie$, extended plate theory of 16th order.

The dispersion curves for the phase frequencies based on the extended plate theory of 16th order using the Legendre polynomials are shown below in Fig. 2 (longitudinal modes) and Fig. 3 (bending modes).

The branches corresponding to both lowest-order longitudinal and bending modes tend to the frequency of the Rayleigh wave, $\omega_R = \kappa\beta_R^{-1}$ where $\beta_R = c_R/c_1$ is the dimensionless Rayleigh wave velocity, as the dimensionless wavenumber tends to infinity, $\kappa \to \infty$. The similar results were obtained in [60] on the background of the "elementary" theory using the Legendre polynomials as well as in [61] on the basis of the "finite layer" model (2.16).

The convergence analysis of the locking frequencies at $\kappa \to 0$ to their exact values is shown in the Table 1 for the longitudinal modes and in the Table 2 for the bending modes.

Table 1. Convergence of the locking frequencies approximation for longitudinal normal modes on the background of the Nth order extended plate theory, $N = 1 \dots 16$, as compared with the exact solution (Ex.); n – mode number; N – order of the plate theory.

N	n									
	1	2	3	4	5	6	7	8	9	10
2	0.00	–	–	–	–	–	–	–	–	–
3	0.00	1.89	–	–	–	–	–	–	–	–
4	0.00	1.89	1.97	–	–	–	–	–	–	–
5	0.00	1.91	1.98	5.68	–	–	–	–	–	–
6	0.00	1.91	2.00	4.03	5.68	–	–	–	–	–
7	0.00	1.91	2.00	4.03	5.74	9.83	–	–	–	–
8	0.00	1.91	2.00	4.02	5.73	6.37	9.82	–	–	–
9	0.00	1.91	2.00	4.02	5.72	6.37	9.64	14.67	–	–
10	0.00	1.91	2.00	4.00	5.72	6.11	9.13	9.64	14.67	–
11	0.00	1.91	2.00	4.00	5.72	6.11	9.13	9.51	13.73	20.40
12	0.00	1.91	2.00	4.00	5.72	6.00	8.35	9.52	12.40	13.73
13	0.00	1.91	2.00	4.00	5.72	6.00	8.35	9.53	12.40	13.32
14	0.00	1.91	2.00	4.00	5.72	6.00	8.00	9.53	10.84	13.32
15	0.00	1.91	2.00	4.00	5.72	6.00	8.00	9.53	10.84	13.34
16	0.00	1.91	2.00	4.00	5.72	6.00	8.00	9.53	10.05	13.34
Ex.	0.00	1.91	2.00	4.00	5.72	6.00	8.00	9.53	10.00	12.00

It can be seen that the extended, or "constrained", plate theory of the 16th order secures the convergence of the 9 lowest phase frequencies of longitudinal modes as well as of the 9 lowest phase frequencies of the bending modes. Thus, it offers the faster convergence as compared with the "elementary" theory; the solution [60] that is based on the Legendre polynomials and neglects the constraints leads to the same approximation errors at $N = 20$. At the same time the unconstrained "finite layer" plate theory secures the convergence of the 10 lowest locking frequencies of longitudinal modes as well as of the 9 lowest locking frequencies of the bending modes at $N = 28$ [61]; the "spectral" element solution based on the linear shape functions (2.16) converges slowly as compared with the one based on the Legendre polynomials [60].

Let us construct the waveforms following from the eigenvectors of the operator (3.6):

Table 2. Convergence of the locking frequencies approximation for bending normal modes on the background of the Nth order extended plate theory. $N = 1 \ldots 16$ as compared with the exact solution (Ex.); n − mode number; N − order of the plate theory.

N	n									
	1	2	3	4	5	6	7	8	9	10
2	0.00	–	–	–	–	–	–	–	–	–
3	0.00	0.99	–	–	–	–	–	–	–	–
4	0.00	0.99	3.77	–	–	–	–	–	–	–
5	0.00	1.00	2.98	3.77	–	–	–	–	–	–
6	0.00	1.00	2.98	3.82	7.68	–	–	–	–	–
7	0.00	1.00	3.00	3.81	5.16	7.68	–	–	–	–
8	0.00	1.00	3.00	3.81	5.16	7.67	12.14	–	–	–
9	0.00	1.00	3.00	3.81	5.06	7.67	7.70	12.14	–	–
10	0.00	1.00	3.00	3.81	5.06	7.62	7.70	11.65	17.41	–
11	0.00	1.00	3.00	3.81	5.00	7.20	7.62	10.70	11.65	17.41
12	0.00	1.00	3.00	3.81	5.00	7.20	7.62	10.70	11.41	15.92
13	0.00	1.00	3.00	3.81	5.00	7.00	7.62	9.56	11.41	14.21
14	0.00	1.00	3.00	3.81	5.00	7.00	7.62	9.56	11.42	14.21
15	0.00	1.00	3.00	3.81	5.00	7.00	7.62	9.00	11.42	12.19
16	0.00	1.00	3.00	3.81	5.00	7.00	7.62	9.00	11.41	12.19
Ex.	0.00	1.00	3.00	3.81	5.00	7.00	7.62	9.00	11.00	11.43

$$(4.2) \quad u_\alpha^n(\zeta) = U_{1,2}^{kn} \mathrm{p}_k(\zeta), \quad [U_1^{kn} \; U_2^{kn}] = \mathbf{U}^n, \quad k = 0, \ldots, N, \; n = 0, \ldots, N.$$

Let us consider the exact solution of the Rayleigh–Lamb problem at $\kappa \to 0$. The symmetric modes are defined as follows:

$$(4.3) \qquad u_1^{n*} = A_{11} \cos \pi m \zeta, \quad u_2 \equiv 0, \quad 2\pi^{-1}\omega = 2m,$$

$$(4.4) \qquad u_1 = 0, \quad u_2^{n*} = A_{12} \sin \pi \frac{2m+1}{2}\zeta, \quad 2\pi^{-1}\omega = (2m+1)\beta^{-1},$$

for $m = 0, 1, 2, \ldots$; while the antisymmetric modes are given by the formulae

$$(4.5) \qquad u_1 \equiv 0, \quad u_2^{n*} = A_{21} \cos \pi m \zeta, \quad \omega = 2\beta^{-1}m, \quad m = 0, 2, \ldots,$$

$$(4.6) \qquad u_1^{n*} = A_{22} \sin \pi \frac{2m+1}{2}\zeta, \quad u_2 \equiv 0, \quad \omega = 2m+1, \quad m = 0, 1, 2 \ldots.$$

Here A_{ij} are arbitrary constants. Thus, the relative error of the approximate waveforms obtained on the background of the Nth order plate theory can be estimated using the norm for the Hilbert space $H[-1, 1]$ taking into account (4.2)–(4.6):

$$\Delta_n = \frac{\|u_\alpha^n(\zeta) - u_\alpha^{n*}(\zeta)\|}{\|u_\alpha^{n*}(\zeta)\|}, \quad \|u_\alpha^n(\zeta)\|^2 = (u_\alpha^n, u_\alpha^n)_1 = \int\limits_{-1}^{1} a^{\alpha\beta} u_\alpha^n(\zeta) u_\beta^n(\zeta) d\zeta.$$

The relative errors of the approximate waveforms are shown below in the Tables 3 and 4 for longitudinal and bending modes respectively.

Table 3. Relative error of approximation of the longitudinal modes at locking frequencies.

N	n								
	2	3	4	5	6	7	8	9	10
1	0.20	–	–	–	–	–	–	–	–
3	0.01	0.40	–	–	–	–	–	–	–
5	0.00	0.03	1.03	1.36	–	–	–	–	–
7	0.00	0.00	0.01	0.21	1.26	–	–	–	–
9	0.00	0.00	0.00	0.01	0.42	1.21	–	–	–
11	0.00	0.00	0.00	0.00	0.10	0.01	1.30	–	–
13	0.00	0.00	0.00	0.00	0.01	0.00	0.76	–	–
15	0.00	0.00	0.00	0.00	0.00	0.00	0.41	1.03	1.39
17	0.00	0.00	0.00	0.00	0.00	0.00	0.14	0.00	0.62
19	0.00	0.00	0.00	0.00	0.00	0.00	0.02	0.00	0.31
21	0.00	0.00	0.00	0.00	0.00	0.00	0.00	0.00	0.09

Table 4. Relative error of approximation of the bending modes at locking frequencies.

N	n								
	2	3	4	5	6	7	8	9	10
1	0.19	–	–	–	–	–	–	–	–
3	0.00	0.52	0.43	–	–	–	–	–	–
5	0.00	0.11	0.03	0.70	–	–	–	–	–
7	0.00	0.01	0.00	0.31	–	–	–	–	–
9	0.00	0.00	0.00	0.06	1.41	1.19	1.21	–	–
11	0.00	0.00	0.00	0.00	0.19	0.00	0.71	–	–
13	0.00	0.00	0.00	0.00	0.02	0.00	0.36	–	–
15	0.00	0.00	0.00	0.00	0.00	0.00	0.10	1.40	1.21
17	0.00	0.00	0.00	0.00	0.00	0.00	0.01	0.24	0.00
19	0.00	0.00	0.00	0.00	0.00	0.00	0.00	0.05	0.00
21	0.00	0.00	0.00	0.00	0.00	0.00	0.00	0.00	0.00

The first four normal waveforms (4.2) obtained on the background of the approximate solution are shown in Fig. 4 (longitudinal waves) and Fig. 5 (bending waves).

(a)

(b)
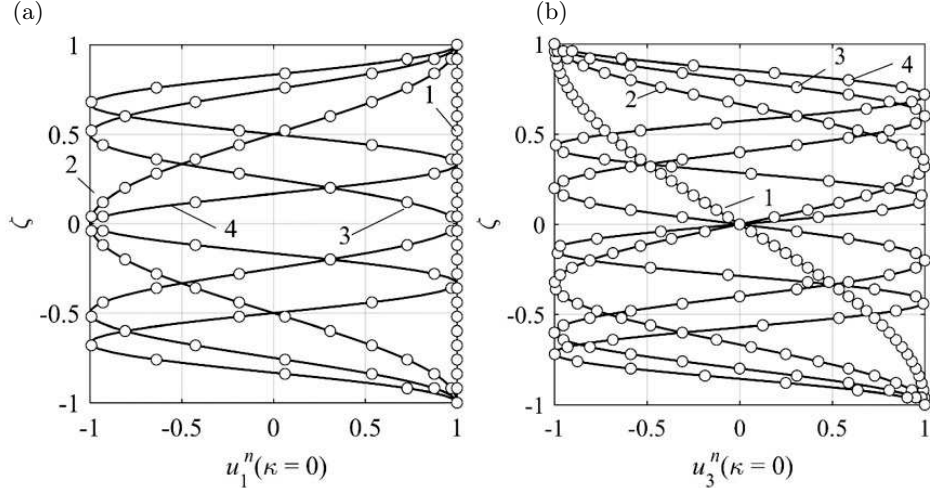
FIG. 4. Dimensionless normal waveforms of longitudinal waves at locking frequencies $(\kappa = 0)$: (a) longitudinal displacement $\tilde{u}_1^n(\zeta)$, $n = 1, \ldots, 4$; (b) transversal displacement $\tilde{u}_3^n(\zeta)$, $n = 1, \ldots, 4$; exact solution (solid lines), extended plate theory of 16th order (dots).

(a)

(b)
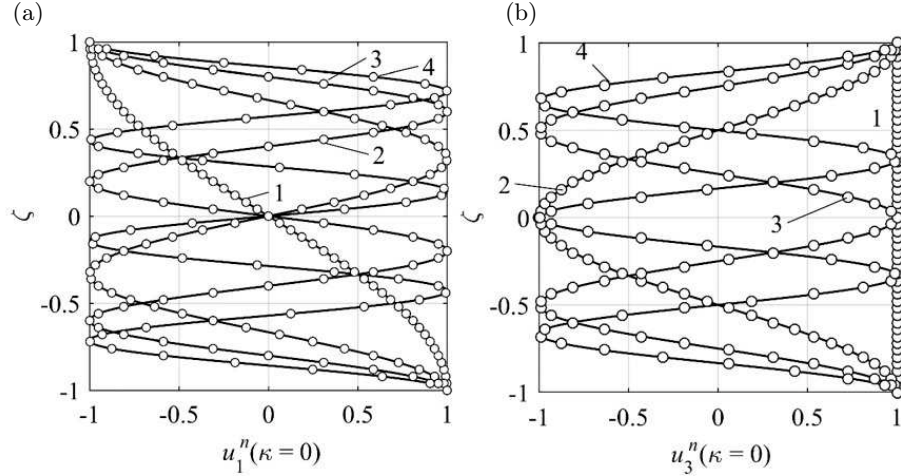
FIG. 5. Dimensionless normal waveforms of bending waves at locking frequencies $(\kappa = 0)$: (a) longitudinal displacement $\tilde{u}_1^n(\zeta)$, $n = 1, \ldots, 4$; (b) transversal displacement $\tilde{u}_3^n(\zeta)$, $n = 1, \ldots, 4$; exact solution (solid lines), extended plate theory of 16th order (dots).

The stress components corresponding to the waveforms (4.2) are given by (4.7):

(4.7)
$$\sigma_{11}(\zeta, K)|_{\kappa=0} = V_{(kn)} \bar{D}_{(m\cdot)}^{(\cdot n)} U_3^{K(m)} \mathrm{p}^{(k)}(\zeta),$$

$$\sigma_{13}(\zeta, K)|_{\kappa=0} = V_{(kn)} \bar{D}_{(m\cdot)}^{(\cdot n)} U_1^{K(m)} \mathrm{p}^{(k)}(\zeta),$$

$$\sigma_{33}(\zeta, K)|_{\kappa=0} = \beta^{-2} V_{(kn)} \bar{D}_{(m\cdot)}^{(\cdot n)} U_3^{K(m)} \mathrm{p}^{(k)}(\zeta).$$

(a)

(b)
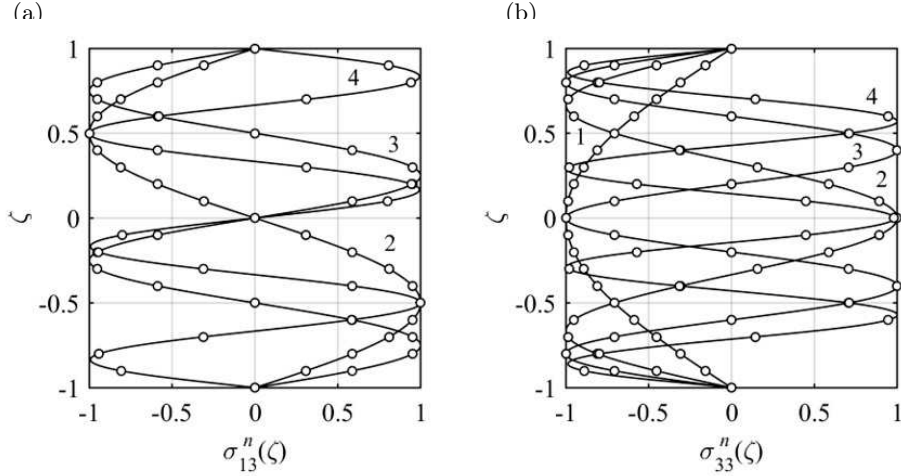
FIG. 6. Normalized distributions of sterss components corresponding to the locking frequencies of longitudial waves: (a) transverse shear stress, $\sigma_{13}^k(\zeta)$; (b) transverse normal stress, $\sigma_{33}^k(\zeta)$: exact solution (solid line), extended plate theory of 16th order (dots).

The normalized distributions of the stresses (4.7), $\sigma_{ij}(\zeta)/\max|\sigma_{ij}(\zeta)|$ ($\zeta \in [-1, 1]$), corresponding to the longitudinal modes of normal waves at $\kappa \to 0$ are presented in Fig. 6. As it could be seen, the extended theory of plates of the Nth order accounting for the constraints (3.8) allows one to fulfil the boundary conditions on the faces of a layer.

For more details see also [26, 60, 61] and [66].

5. Modelling of normal wave dispersion in functionally graded plates

Let the plate be graded symmetrically with respect to its mid-plane, i.e. the "two-sided" functionally graded structure with the ceramics volume ratio according to the power law (5.1) is considered below:

$$(5.1) \qquad\qquad q(\zeta) = |\zeta|^P P \in \mathbb{R}_+ \cup \{0\}.$$

The variations of the Young modulus and the mass density across the plate thickness are given by the formulae (3.1), (3.2). Let us consider a material with two constituents [65], an Aluminium phase with the Young modulus $E_{\text{M}} = 7.0 \times 10^{10}$ Pa and a phase of Al_2O_3 ceramics with the Young modulus $E_{\text{C}} = 3.8 \times 10^{11}$ Pa. The mass densities of these phases are equal to $\rho_{\text{C}} = 4000$ kg/m^3 and $\rho_M = 2700$ kg/m^3, respectively, while the Poisson ratio is equal to 0.31 for both phases.

The further investigation is based on the extended plate theory of 18th order. The dependencies of the locking frequencies obtained with Legendre polynomials

as base functions $p_{(k)}(\zeta)$ on the power law index P are shown in the Table 5 (longitudinal modes) and in the Table 6 (bending modes).

Table 5. Dimensionless locking frequencies of the longitudinal modes in the symmetrically graded metal-ceramic plates with various power law indices P.

P	n								
	2	3	4	5	6	7	8	9	10
0	1.91	2.00	4.00	5.72	6.00	8.00	9.53	10.00	12.05
1	1.22	1.64	3.20	4.45	4.79	6.41	7.52	8.18	10.36
2	1.05	1.36	2.77	3.94	4.17	5.60	6.62	7.21	9.31
3	1.00	1.22	2.57	3.64	3.88	5.19	6.15	6.64	8.64
4	0.98	1.15	2.45	3.45	3.71	4.96	5.87	6.29	8.21
5	0.97	1.10	2.37	3.31	3.59	4.81	5.68	6.07	7.83
6	0.96	1.08	2.30	3.22	3.51	4.71	5.55	5.92	7.54
7	0.96	1.06	2.26	3.16	3.45	4.63	5.44	5.81	7.32
8	0.96	1.05	2.22	3.11	3.40	4.57	5.36	5.73	7.16
9	0.96	1.04	2.20	3.08	3.36	4.52	5.30	5.67	7.03
10	0.96	1.04	2.17	3.05	3.33	4.48	5.24	5.62	6.93

Table 6. Dimensionless locking frequencies of the bending modes in symmetrically graded metal-ceramic plates with various power law indices P.

P	n								
	2	3	4	5	6	7	8	9	10
0	1.00	3.00	3.81	5.00	7.00	7.62	9.00	11.02	11.43
1	0.64	2.33	3.12	3.95	5.57	6.10	7.30	9.12	9.36
2	0.55	2.07	2.59	3.47	4.88	5.28	6.42	7.95	8.43
3	0.52	1.91	2.32	3.23	4.54	4.90	5.92	7.40	7.79
4	0.51	1.81	2.18	3.08	4.34	4.67	5.62	7.07	7.34
5	0.51	1.74	2.10	2.98	4.21	4.51	5.43	6.85	7.01
6	0.51	1.69	2.05	2.91	4.11	4.39	5.31	6.69	6.77
7	0.51	1.66	2.02	2.86	4.04	4.31	5.22	6.57	6.59
8	0.51	1.63	2.00	2.81	3.99	4.24	5.15	6.45	6.48
9	0.51	1.61	1.99	2.78	3.94	4.19	5.09	6.35	6.41
10	0.51	1.60	1.98	2.75	3.90	4.14	5.05	6.27	6.34

Finally, let us consider the asymmetrically graded plate with the ceramics volume ratio according to the power law (5.2):

$$(5.2) \qquad\qquad q(\zeta) = 2^{-p}(1 + \zeta)^p.$$

The dependencies of the locking frequencies obtained with Legendre polynomials as base functions $p_{(k)}(\zeta)$ on the power law index P are shown below in the Table 7.

Table 7. Dimensionless locking frequencies in asymmetrically graded metal-ceramic plates with various power law indices P.

P	n								
	2	3	4	5	6	7	8	9	10
0	1.00	1.91	2.00	3.00	3.81	4.00	5.00	5.72	6.00
1	0.81	1.54	1.58	2.36	3.01	3.14	3.92	4.49	4.70
2	0.67	1.27	1.36	2.05	2.59	2.73	3.42	3.90	4.11
3	0.60	1.14	1.26	1.90	2.40	2.54	3.18	3.63	3.82
4	0.56	1.07	1.20	1.82	2.28	2.43	3.04	3.46	3.65
5	0.54	1.03	1.16	1.76	2.21	2.35	2.95	3.35	3.54
6	0.53	1.00	1.13	1.72	2.15	2.30	2.88	3.27	3.47
7	0.52	0.99	1.10	1.69	2.10	2.26	2.84	3.21	3.41
8	0.52	0.98	1.09	1.66	2.07	2.23	2.80	3.17	3.36
9	0.51	0.97	1.07	1.64	2.05	2.21	2.77	3.13	3.33
10	0.51	0.97	1.06	1.63	2.03	2.19	2.74	3.10	3.30

The presented results shows that the locking frequencies for power graded waveguides of both symmetric and asymmetric structures drop, but the lowest frequencies almost converge at power law indices exceeding 10 when the material becomes "skinned" with only small ceramic-rich layers near plate faces; contrarily, for the prevailing high-modulus ceramics and thin metal "skins" the phase frequencies raise [61]. The convergence is faster than the one corresponding to the "spectral" element plate model used in [61] and [68].

6. Conclusions

The extended higher-order theory of heterogeneous elastic plates based on the Lagrangian formalism of analytical dynamics of continuum systems is applied to investigate the normal wave dispersion in plane waveguides. The "extended" model of a plate of Nth order interprets the boundary conditions shifted from the faces onto the base surface as supplementary constraints for the variational formulation of two-dimensional models and allows one to fulfil the boundary conditions exactly. The obtained unified formulation is common with various base functions, as well as the Legendre polynimials, as the finite element discretization of the plate across the thickness, as the Shauder base system. The corresponding constrained spectral problem for the plate is formulated as a stationary values problem for two quadratic forms, and its solution based on the

Golub approach is proposed. The analysis of the convergence of the locking frequencies and the corresponding wave forms obtained from the approximate solutions based on the higher-order theories is performed for a homogeneous isotropic plate using the exact solution of the Rayleigh–Lamb problem as a reference one.

The solution for the problem of the dispersion of normal waves is obtained for the functionally graded waveguide with two constituents, the metal and the ceramics, with both symmetric and asymmetric power-law variation of the ceramic volume fraction across the thickness for several power law indices. The locking phase frequencies are computed. It is shown that for power graded plates the dimensionless locking frequencies drop as the power law index rises and the high-modulus ceramic constituent prevails, and their convergence for lowest frequencies is observed for $P, \dots, 10$, i.e. for "skinned" power-graded structures with thin ceramic-rich layers near the faces.

The proposed approach could be used for the analysis of the impact of various uncertainties of functionally graded material structures on the dispersion properties of waveguides as well as to solve inverse coefficient problems of stationary dynamics being a base for non-destructive testing methods.

Acknowledgements

References

1. M. Koizumi, *The concept of FGM*, Ceramic Transactions. Functionally Gradient Materials, **34**, 3–10, 1993.

2. N. Noda, *Thermal stresses in materials with temperature-dependent properties*, Applied Mechanics Reviews, **44**, 383–397, 1991.

3. G.N. Praveen, J.N. Reddy, *Nonlinar transient thermoelastic analysis of functionally graded ceramic/metal plates*, International Journal of Solids and Structures, **35**, 33, 4457–4476, 1998.

4. G.M. Kulikov, S.V. Plotnikova, *Three-dimensional solution of the free vibration problem for metal-ceramics shells using the Method of Sampling Surfaces*, Mechanics of Composite Materials, **53**, 1, 31–44, 2017.

5. S.S. Pendhari, M.P. Mahajan, T. Kant, *Static analysis of functionally graded laminates according to power-law variation of elastic modulus under bidirectional bending*, International Journal of Computational Methods, **14**, 5, p. 1750055, 2017.

6. F.Z. Zaoui, A. Tounsi, D. Quinas, *Free vibration of functionally graded plates resting on elastic foundations based on quasi-3D hybrid-type higher order shear deformation theory*, Smart Structures and Systems, **20**, 4, 509–524, 2017.

7. H. Altenbach, V.A. Eremeyev, *Eigen-vibrations of Plates made of Functionally Graded Material*, Computers, Materials, Continua, **9**, 2, 153–177, 2009.

8. L. Lu, M. Chekroun, O. Abraham, V. Maupin, *Mechanical properties estimation of functionally graded materials using surfece waves recorded with a laser interferometer*, Independent Nondestructive Testing and Evaluation International, **44**, 2, 169–177, 2011.

9. J. Yu, B. Wu, *The inverse of maerial properties of functionally graded pipes using the dispersion of guided waves and an artificial neural network*, Independent Nondestructive Testing and Evaluation International, **42**, 5, 452–468, 2009.

10. M. Sale, P. Rizzo, A. Marzani, *Semi-analytical formulation for the uided waves-based reconstruction of elastic moduli*, Mechanical Systems and Signal Processing, **25**, 6, 2241–2256, 2011.

11. R. Nedin, S. Nesterov, A. Vatulyan, *On reconstruction of thermalphysic characteristics of functionally graded hollow cylinders*, Applied Mathematical Modelling, **40**, 4, 2711–2719, 2016.

12. Z.-Q. Chang, R.C. Batra, *Three-dimensional thermoelastic deformations of a functionally graded elliptic plate*, Composites: Part B. Engineering, **31**, 97–106, 2000.

13. Z.-Q. Cheng, J.N. Reddy, *Three-dimensional thermoelastic deformations of functionally graded rectengular plates*, European Journal of Mechanics A/Solids, **20**, 841–855, 2001.

14. J.N. Reddy, Z.-Q. Cheng, *Three dimensional solutions of smart functionally graded plates*, Journal of Applied Mechanics, **68**, 234–241, 2001.

15. S. Brischetto, *A closed-form 3D-shell solution for multilayered structures subjected to different load combinations*, Aerospace Science and Technology, **70**, 29–46, 2017.

16. S. Brischetto, *A general exact elastic shell solution for bending analysis of functionally graded materials*, Composite Structures, **175**, 70–85, 2017.

17. S. Brischetto, *Exact three-dimensional static analysis of single- and multi-layered plates and shells*, Composites: Part B. Engineering, **119**, 230–252, 2017.

18. C.C. Vel, R.C. Batra, *Three-dimensional exact solution for the vibration of functionally graded rectangular plates*, Journal of Sound and Vibration, **272**, 703–730, 2004.

19. S. Brischetto, E. Carrera, *Importance of igher order modes and refined theories in free vibration analysis of composite plates*, Journal of Applied Mechanics, **77**, 1, Article no. 011013 (14 pages), 2010.

20. R.C. Batra, S. Aimmanee, *Vibrations of thick isotropic plates with higher-order shear and normal deformable plate theories*, Computers & Structures, **83**, 12–13, 934–955, 2005.

21. J.-H. Kang, A.W. Leissa, *Three-dimensional vibration analysis of thick, complete conical shells*, Journal of Applied Mechanics, **71**, 6, 502–507, 2004.

22. H. Altenbach, *On the determination of transverse shear stiffness of orthotropic plates*, Zeitschrift für Angewandte Mathematik und Physik, **51**, 629–649, 2000.

23. H. Altenbach, *An alternative determination of transverse shear stiffness for sandwich and laminated plates*, International Journal of Solids and Structures, **37**, 25, 3503–3520, 2000.

24. I.N. VEKUA, *Shell Theories: General Methods of Construction*, Pitman Advanced Publishing Program, Boston, 1985.

25. V.V. ZOZULYA, *A higher order theory for shells, plates and rods*, International Journal of Mechanical Sciences, **103**, 40–54, 2015.

26. S.I. ZHAVORONOK, *A Vekua-type linear theory of thick elastic shells*, ZAMM – Journal of Applied Mathematics and Mechanics/Zeitschrift für Angewandte Mathematik und Mechanik, **94**, 1–2, 164–184, 2014.

27. V.V. ZOZULYA, C. CHANG, *A high order theory for functionally graded axisymmetric cylindrical shells*, International Journal of Mechanical Science, **60**, 1, 12–22, 2012.

28. A. GUPTA, M. TALHA, *An assessment of a non-polynomial based higher order shear and normal deformation theory for vibration response of gradient plates with initial geometric imperfections*, Composites Part B: Engineering, **107**, 1, 141–161, 2016.

29. A. GUPTA, M. TALHA, B.N. SINGH, *Vibration characteristics of functionally graded material plate with various boundary constraints using higher order shear deformation theory*, Composites Part B: Engineering, **94**, 1, 64–74, 2016.

30. S.A. SHEIKHOLESLAMI, A.R. SAIDI, *Vibration analysis of functionally graded rectangular plates resting on elastic foundation using higher-order shear and normal deformable plate theory*, Composite Structures, **106**, 350–361, 2013.

31. M. MEHRKASH, M. AZKARI, H.R. MIRDAMADI, *Reliability assessment of different plate theories for elastic wave propagation analysis in functionally graded plates*, Ultrasonics, **54**, 1, 106–120, 2014.

32. A.L. GOLDENVEIZER, J.D. KAPLUNOV, *Dynamic boundary layers in problems of vibrations of shells*, Mechanics of Solids, **23**, 4, 146–155, 1988.

33. J.D. KAPLUNOV, L.YU. KOSSOVICH, E.V. NOLDE, *Dynamics of thin-walled elastic bodies*, Academic Press, San Diego, London, Boston, New York, Sydney, Tokyo, Toronto, 1998.

34. X. CAO, J. JIN, Y. RU, J. SHI, *Asymptotic analytical solution for horizontal shear waves in a piezoelectric elliptic culinder shell*, Acta Mechanica, **226**, 10, 3387–3400, 2015.

35. D. GORDEZIANI, M. AVALISHVILI, G. AVALISHVILI, *Hierarchical models for elastic shells in curvilinear coordinates*, Computers & Mathematics with Applications, **51**, 1789–1808, 2006.

36. C. SCHWAB, S. WRIGHT, *Boundary layers of hierarchical beam and plate models*, Journal of Elasticity, **38**, 1–40, 1995.

37. A. IDESMAN, *Accurate finite-element modeling of wave propagation in composite and functionally graded materials*, Composite Structures, **117**, 298–308, 2014.

38. A.M.A. NEVES, A.J.M. FERREIRA, E. CARRERA, M. CINEFRA, C.M.C. ROQUE, R.M.N. JORGE, C.M.M. SOARES, *Static, free vibration and buckling analysis of isotropic and sandwich functionally graded plates using a quasi-3D higher-order shear deformation theory and a meshless technique*, Composites Part B: Engineering, **44**, 1, 657–674, 2013.

39. B.D. ANNIN, Y.M. VOLCHKOV, *Nonclassical models of the theory of plates and shells*, Journal of Applied Mechanics and Technical Physics, **57**, 5, 769–776, 2016.

40. R. KIENZLER, P. SCHNEIDER, *Consistent theories of isotropic and anisotropic plates*, Journal of Theoretical and Applied Mechanics, **50**, 3, 755–768, 2012.

41. X. CAO, F. JIN, I. JEON, *Calculation of propagation properties of Lamb waves in a functionally graded material (FGM) plate by power series technique*, Independent Nondestructive Testing and Evaluation International, **44**, 1, 84–92, 2011.

42. D. ZHOU, F.T.K. AU, Y.K. CHEUNG, S.H. LO, *Three-dimensional vibration analysis of circular and annular plates via the Chebyshev–Ritz method*, International Journal of Solids and Structures, **40**, 3089–3105, 2003.

43. L. ELMAIMOUNI, J.E. LEFEBVRE, V. ZHANG, T. GRYBA, *Guided waves in radially graded cylinders: a polynomial approach*, Independent Nondestructive Testing and Evaluation International, **38**, 5, 344–353, 2005.

44. L. ELMAIMOUNI, J.E. LEFEBVRE, F.E. RATOLOJANAHARY, A. RAHERISON, T. GRYBA, J. CARLIER, *Modal analysis and harmonic response of resonators: An extension of a mapped orthogonal functions technique*, Wave Motion, **48**, 1, 93–104, 2011.

45. J.G. YU, C. ZHANG, J.E. LEFEBVRE, *Guided wave characteristics in functionally graded piezoelectric rings with rectangular cross-sections*, Acta Mechanica, **226**, 3, 597–609, 2015.

46. J. YU, J.E. LEFEBVRE, L. ELMAIMOUNI, *Guided waves in multilayered plates: An improved orthogonal polynoial approach*, Acta Mechanica Solida Sinica, **27**, 5, 542–550, 2014.

47. M. ZHENG, S. HE, Y. LU, B. WU, *State-vector formalism and the Legendre polynomial solution for modelling guided waves in anisotropic plates*, Journal of Sound and Vibration, **412**, 372–388, 2018.

48. G.M. KULIKOV, S.V. PLOTNIKOVA, *Strong sampling surfaces formulation for laminated composite plates*, Composite Structures, **172**, 73–82, 2017.

49. G.M. KULIKOV, S.V. PLOTNIKOVA, *Strong sampling surfaces formulation for layered shells*, International Journal of Solids and Structures, **121**, 75–85, 2017.

50. G.M. KULIKOV, S.V. PLOTNIKOVA, *Three-dimensional analysis of metal-ceramics shells by the method of sampling surfaces*, Mechanics of Composite Materials, **51**, 4, 455–464, 2015.

51. G.M. KULIKOV, S.V. PLOTNIKOVA, *Three-dimensional exact analysis of piezoelectric laminated plates via a sampling surfaces method*, International Journal of Solids and Structures, **50**, 11–12, 1916–1929, 2013.

52. G.M. KULIKOV, E. CARRERA, S.V. PLOTNIKOVA, *Hybrid-mixed quadrilateral element for laminated plates composed of functionally graded materials*, Advanced Materials and Technologies, **1**, 14–55, 2017.

53. G.M. KULIKOV, S.V. PLOTNIKOVA, *Three-dimensional exact analysis of functionally graded laminated composite materials*, Advanced Structured Materials, **45**, 223–241, 2015.

54. Y.M. VOLCHKOV, L.A. DERGILEVA, *Reducing three-dimensional elasticity problems to two-dimensional problems by approximating stresses and displacements by Legendre polynomials*, Journal of Applied Mechanics and Technical Physics, **48**, 3, 450–459, 2007.

55. A.A. AMOSOV, S.I. ZHAVORONOK, *An approximate high-order theory of thick anisotropic shells*, International Journal for Computational Civil and Structural Engineering, **1**, 5, 28–38, 2003.

56. S.I. ZHAVORONOK, A.N. LEONTIEV, K.A. LEONTIEV, *Analysis of thick-walled rotation shells based on the Legendre polynomials*, International Journal for Computational Civil and Structural Engineering, **6**, 1–2, 105–111, 2010.

57. S.I. ZHAVORONOK, *Variational formulations of Vekua-type shell theories and some their applications*, Shell Structures: Theory and Applications, **3**, 341–344, 2014.

58. S.I. ZHAVORONOK, *On the variational formulation of the extended thick anisotropic shells theory of I.N. Vekua type*, Procedia Enginering, **111**, 888–895, 2015.

59. S.I. ZHAVORONOK, *A general higher-order shell theory based on the analytical dynamics of constrained continuum systems*, Shell Structures: Theory and Applications, **4**, 189–192, 2017.

60. E.L. KUZNETSOVA, E.L. KUZNETSOVA, L.N. RABINSKIY, S.I. ZHAVORONOK, *On the equations of the analytical dynamics of the quasi-3D plate theory of I.N. Vekua type and some their solutions*, Journal of Vibroengineering, **20**, 2, 1108–1117, 2018.

61. O.V. EGOROVA, A.S. KURBATOV, L.N. RABINSKIY, S.I. ZHAVORONOK, *Modeling of the dynamics of plane functionally graded waveguides based on the different formulations of the plate theory of I.N. Vekua type*, Mechanics of Advanced Materials and Structures, 2019, DOI: 10.1080/15376494.2019.1578008.

62. P.A. ZHILIN, *Mechanics of deformable directed surfaces*, International Journal of Solids and Structures, **12**, 635–648, 1976.

63. H. ALTENBACH, V. EREMEYEV, *On the linear theory of micropolar plates*, ZAMM – Journal of Applied Mathematics and Mechanics/Zeitschrift für Angewandte Mathematik und Mechanik, **89**, 4, 242–256, 2009.

64. W. PIETRASZKIEWICZ, V. KONOPINSKA, *On unique kinematics for the branching shells*, International Journal of Solids and Structures, **48**, 2238–2244, 2011.

65. H. MATSUNAGA, *Free vibration and stability of functionally graded plates according to a 2D higher-order deformation theory*, Composite Structures, **82**, 499–512, 2008.

66. S.I. ZHAVORONOK, *On the use of extended plate theories of Vekua-Amosov type for vave dispersion problems*, International Journal for Computational Civil and Structural Engineering, **14**, 1, 36–48, 2018.

67. G.H. GOLUB, R. UNDERWOOD, *Stationary value of the ratio of quadratic forms subject to linear constraints*, 1969.

68. L.N. RABINSKIY, S.A. SITNIKOV, *Development of technologies for obtaining composite material based on silicone binder for its further use in space electric rocket engines*, Periodico Tche Quimica, 15, Special Issue 1, 390–395.